Effect of xylitol on low-density lipoprotein-stimulated oxidative stress in THP-1 cells

ZILE HUANG[1*], ANKE LI[1*], RUI HUANG[2*], MENGMENG SHI[1], RUJING YANG[1], WENYAN WANG[1], ZHEN HUANG[1], YANHONG LIU[3] and JUNZHU WU[1]

[1]Taikang Medical School, School of Basic Medical Sciences, Wuhan University, Wuhan, Hubei 430072, P.R. China; [2]Department of Ophthalmology, Zhongnan Hospital of Wuhan University, Wuhan, Hubei 430071, P.R. China; [3]Department of Clinical Laboratory, Institute of Translational Medicine, Renmin Hospital of Wuhan University, Wuhan, Hubei 430060, P.R. China

Received December 17, 2024; Accepted April 3, 2025

DOI: 10.3892/mmr.2025.13555

Abstract. Atherosclerosis (AS) is a chronic inflammatory disease caused by oxidative stress and the oxidation of low-density lipoprotein (LDL). Xylitol, a widely used sugar substitute, has antioxidant potential; however, its effects on LDL-induced oxidative stress in AS remain unclear. Using western blot, reverse transcription-quantitative PCR, flow cytometry and so on, the present study investigated the role of xylitol in mitigating oxidative stress induced by high levels of LDL in Tohoku Hospital Pediatrics-1 (THP-1) human monocytic cell line), a model for studying AS. Xylitol significantly alleviated high LDL-induced oxidative stress in THP-1 cells and decreased reactive oxygen species levels, malondialdehyde content and the expression of NADPH oxidase family enzymes. Concurrently, xylitol enhanced the activity and expression of superoxide dismutase and increased the glutathione levels. Mechanistically, xylitol activated the nuclear factor erythroid 2-related factor 2 (Nrf2)/heme oxygenase-1 (HO-1) axis by increasing the NADPH/$NADP^+$ ratio via the regulation of the pentose phosphate pathway via the Nrf2 transcription factor. This led to a decrease in LDL oxidative modification in THP-1 cells (Figs. 6,7). Overall, xylitol attenuates high LDL level-induced oxidative stress in THP-1 cells by modulating the Nrf2-mediated pentose phosphate pathway and activating the Nrf2/HO-1 axis, highlighting its potential for the prevention and treatment of AS.

Correspondence to: Professor Junzhu Wu, Taikang Medical School, School of Basic Medical Sciences, Wuhan University, 115 Donghu Road, Wuchang, Wuhan, Hubei 430072, P.R. China
E-mail: wujunzhu@whu.edu.cn

Professor Yanhong Liu, Department of Clinical Laboratory, Institute of Translational Medicine, Renmin Hospital of Wuhan University, 99 Zhangzhidong Road, Wuhan, Hubei 430060, P.R. China
E-mail: 1376090683@qq.com

*Contributed equally

Abbreviations: AS, Atherosclerosis; THP-1, Tohoku Hospital Pediatrics-1; GO, Gene Ontology; KEGG, Kyoto Encyclopedia of Genes and Genomes; GSEA, Gene Set Enrichment Analysis; GEO, Gene Expression Omnibus; DCFH-DA, dichlorodihydrofluorescein diacetate; G6PD, glucose-6-phosphate dehydrogenase; HO-1, heme oxygenase 1; LDL, low-density lipoprotein; PGD, phosphogluconate dehydrogenase; PPP, pentose phosphate pathway; TKT, transketolase; ROS, reactive oxygen species; CCK-8, Cell Counting Kit-8; MDA, malondialdehyde; GSH, glutathione; SOD, superoxide dismutase; RT-q, reverse transcription-quantitative; ES, enrichment score; KEAP1, kelch-like ECH-associated protein 1

Key words: oxidation of low-density lipoprotein, xylitol, oxidative stress, atherosclerosis, Nrf2

Introduction

Atherosclerosis (AS) is one of the most common causes of cardiovascular disease (1), responsible for ~62% of global cardiovascular disease-associated mortality (23.6 million deaths annually), as reported in the 2025 American Heart Association Heart Disease and Stroke Statistics (2). AS is a multifactorial chronic inflammatory disease in which lipids, inflammatory and smooth muscle cells and necrotic cell debris accumulate in the arterial intima and low-density lipoprotein (LDL) accumulates under the endothelium, forming atheromatous lipid-containing necrotic foci that promote the AS process (3). Its occurrence is associated with dyslipidemia, lipid metabolism dysfunction, smoking and obesity (4). Elevated LDL cholesterol levels caused by lipid metabolism disorders are a key risk factor for AS, as concentrations >0.5-1.0 mmol/l (20-40 mg/dl) increase the likelihood of LDL retention in the intima in a dose-dependent manner, promoting the initiation and progression of AS plaques and markedly raising the risk of cardiovascular disease (5). LDL oxidative modification is a key promoter of AS (6). Studies have shown that oxidized LDL promotes reactive oxygen species (ROS) production in endothelial and smooth muscle cells and macrophages, inhibits endothelial nitric oxide synthase activity in endothelial cells and enhances platelet activity (7,8). Therefore, the decrease of ROS levels and enhancing antioxidant capacity, particularly by mitigating the oxidative modification of LDL, serve a key role in the prevention and treatment of AS.

Xylitol is a sweetener that is often used as a substitute for glucose and is naturally present in fruits and vegetables. Studies have revealed that xylitol can markedly prevent dental caries and decrease gum inflammation (9). Additionally, xylitol has been found to decrease postprandial hyperglycemia, which can help manage diabetes, obesity and metabolic syndrome (10). Chukwuma and Islam (11) demonstrated that xylitol exerts antioxidant effects by increasing expression of antioxidant enzymes in normal rats and in rats with type 2 diabetes, suggesting the antioxidant potential of xylitol. The pentose phosphate pathway (PPP) is a glucose-oxidizing pathway that produces ribose 5-phosphate and NADPH (Fig. 1) (12). Xylitol is also involved in PPP metabolism through the polyol pathway, and PPP serves a key role in suppressing oxidative stress through NADPH (13). Oxidative stress is a key factor in the development of AS. By decreasing the levels of oxidative stress (14), xylitol may help attenuate the progression of AS. The present study aimed to assess whether xylitol mitigates oxidative stress in AS cell models and influences LDL oxidation and to elucidate the underlying molecular mechanisms.

Materials and methods

Cells, culture and treatment. Tohoku Hospital Pediatrics-1 (THP-1) cells, a human monocyte cell line, were supplied by Procell Life Science & Technology Co., Ltd., and verified by STR analysis. THP-1 cells between passages 4 and 10 post-thawing were used. THP-1 cells were maintained as suspension cultures and subcultured at 90% confluence (approximately $1x10^6$ cells/ml) by replacing half of the spent medium with fresh complete medium. THP-1 cells at a density of 70% were divided into three groups: Untreated control, model (100 μg/ml LDL) and experimental (100 μg/ml LDL + 100 mM xylitol; molecular weight, 152.146 g/mol, Cat#B20885; Shanghai Yuanye Biotechnology Co., Ltd.). THP-1 specialized medium was purchased from Procell Life Science & Technology Co., Ltd.

Bioinformatics analysis. Raw gene expression profile of dataset GSE54666 was downloaded from the Gene Expression Omnibus (GEO; ncbi.nlm.nih.gov/geo/). The GSE54666 dataset is a transcriptomic dataset collected using Illumina gene microarrays after treating primary human monocyte-derived macrophages with oxidized LDL for 48 h. This dataset was used to screen for differentially expressed genes associated with AS to explore potential molecular mechanisms.

To extract key information from the gene expression microarray, the AnnoProbe package in R software (R-project.org; version 4.2.3) was used to convert probe IDs into gene symbols. If a gene symbol corresponded to multiple probe IDs, the average expression of the probes was calculated as the representative expression of the gene. Group analysis was performed using Python software (version 3.8.5; python.org/downloads/release/python-385/) and the limma package (v3.46.0) in R, with screening thresholds set at fold change ≥1.5 and $P<0.05$. Subsequently, the clusterProfiler package was used for Gene Ontology (GO; geneontology.org/) and Kyoto Encyclopedia of Genes and Genomes (KEGG; enome.jp/kegg/) enrichment analyses, as well as gene set enrichment analysis (GSEA; gsea-msigdb.org/gsea/index.jsp). Finally, the ggplot2 package (version 3.3.5; ggplot2.tidyverse.org) was used for visualization.

Hoechst 33342/PI staining. Cells were fixed with 4% paraformaldehyde (PFA) (Sigma-Aldrich) at room temperature for 15 min. A total of 1 ml working solution per sample was prepared, consisting of 5 μl each PI and Hoechst 33342 staining solution (Beijing Solarbio Science & Technology Co., Ltd.) and 990 μl RPMI-1640 medium (Gibco). Cells were centrifuged at 8,000 x g for 2 min at 4˚C, the medium was discarded and the cells were resuspended in working solution then incubated in a 37˚C cell culture incubator for 20 min. The cells were washed twice with PBS and resuspended in 100 μl PBS. A 10 μl aliquot of the resuspended cell solution was carefully placed on a glass slide and examined under a fluorescence microscope (Olympus IX73) at 200x magnification.

Cell Counting Kit-8 (CCK-8) assay. Cells were plated in 96-well plates at a density of ~5,000 cells/well and cultured at 37˚C in a 5% CO_2 humidified incubator. The cells were then treated with xylitol at concentrations of 25, 50, 100, 200 and 400 mM. After 24 h, 10 μl CCK-8 reagent (Beijing Solarbio Science & Technology Co., Ltd.) was added for 2.5 h. The absorbance (A) at 450 nm was detected using an EON microplate reader (BioTek Instruments, Inc.) Cell viability was calculated as follows: Cell viability=$(A_{test}-A_{blank})/(A_{control}-A_{blank})$.

Western blot analysis. THP-1 cells were washed with PBS three times and lysed to extract total protein using RIPA lysis buffer (Beyotime Institute of Biotechnology; containing 1% protease and phosphatase inhibitor cocktail and 1 mmol/l PMSF). Following protein quantification using the BCA method, an equal volume of 2X loading buffer was added, followed by mixing boiling at 100˚C and denaturation for 10 min, immediately cooled on ice, and stored at -20˚C until further use. A total of 30 μg protein lysate per lane was separated using 8-15% gels by SDS-PAGE, transferred to a PVDF membrane, blocked with 5% skimmed milk in TBST (0.1% Tween-20) for 2 h at 25˚C, the membranes were incubated with primary antibodies (Table I; β-actin, 1:2,000; all others 1:800) overnight at 4˚C. The membrane was washed four times with 1X TBST for 10 min each time, and horseradish peroxidase (HRP)-conjugated secondary antibody (1:10,000) was added at room temperature for 2 h. After washing four times with 1X TBST, ECL (Beyotime Institute of Biotechnology, Cat#P0018S) was used for advanced development. β-actin was used as the internal reference protein and the gray values of protein bands were analyzed using ImageJ software 1.53 (National Institutes of Health).

Malondialdehyde (MDA), glutathione (GSH) and ROS assay. MDA content was quantified using a commercial assay kit (Beyotime Institute of Biotechnology, Cat# S0131S) based on the chromogenic reaction between MDA) and thiobarbituric acid followed by colorimetric analysis, according to the manufacturer's protocol. The absorbance was measured at 532 nm using the EON microplate reader (Sartorius) and a standard curve was plotted to calculate the MDA content.

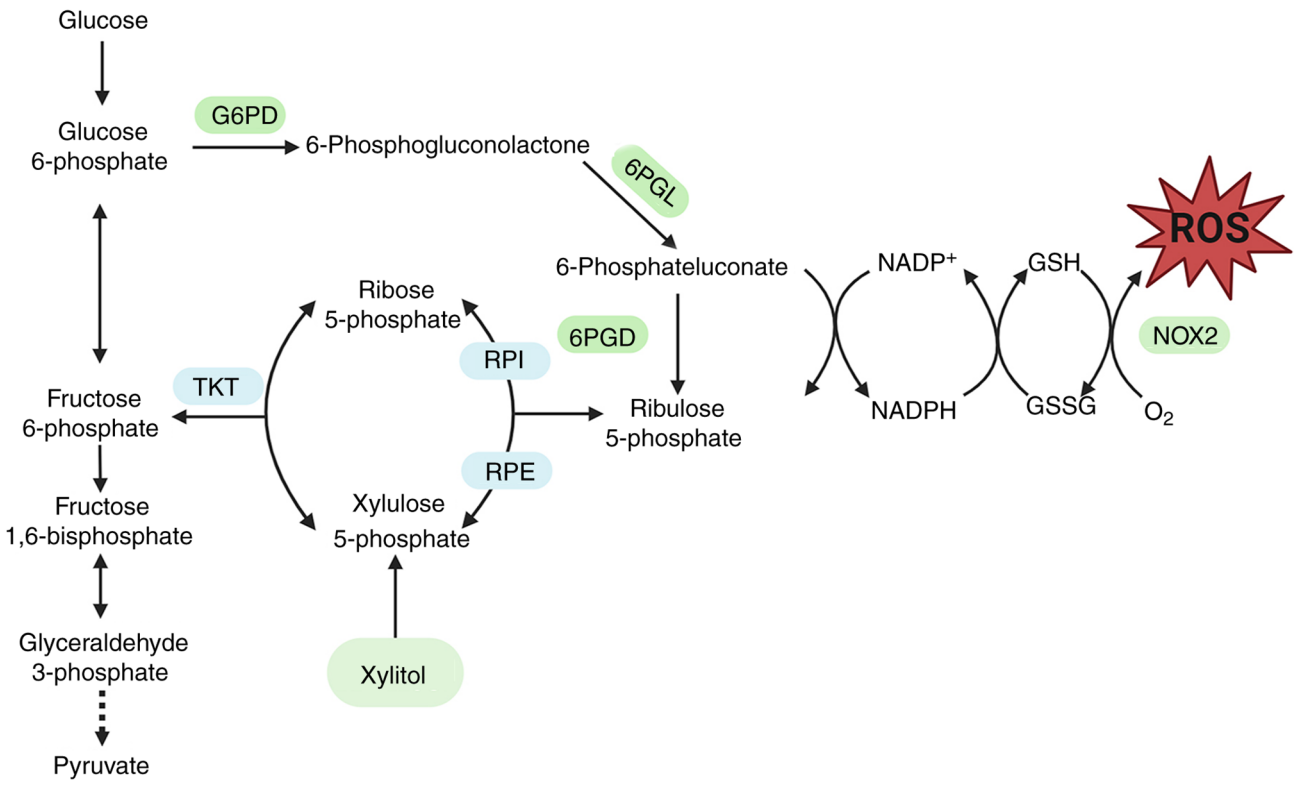

Figure 1. Metabolites and enzymes in glycolysis and oxidative PPP. Xylitol activates the PPP by upregulating the expression of key enzymes, thereby influencing oxidative stress. ROS, reactive oxygen species; G6PD, glucose-6-phosphate dehydrogenase; TKT, transketolase; 6PGL, 6-phosphogluconolactonase; RPI, ribose 5-phosphate isomerase; RPE, ribulose 5-phosphate epimerase; GSH, glutathione; GSSG, glutathione disulfide; PPP, pentose phosphate pathway.

GSH content was measured using a GSH assay kit (Beijing Solarbio Science & Technology Co., Ltd.; cat. no. BC1175) according to the manufacturer's instructions (Beijing Solarbio Science & Technology Co., Ltd.). The absorbance was measured at 412 nm using the EON microplate reader and a standard curve was plotted to calculate the GSH content of the samples.

Dichlorodihydrofluorescein diacetate (DCFH-DA) was diluted in serum-free RPMI-1640 at a ratio of 1:2,000. Cells were resuspended in the diluted DCFH-DA solution at a concentration of ~5x10^6 cells/ml, followed by incubation at 37˚C for 20 min. During incubation, the cells were gently mixed every 3-5 min. Cells were washed with PBS three times and the fluorescence intensity was measured using a CytoFLEX flow cytometry (Beckman Coulter, Model: CytoFLEX S; Software: CytExpert 2.4; beckmancoulter.com/products/flow-cytometry/cytoflex/software) to detect ROS levels.

Measurement of superoxide dismutase (SOD) and glucose-6-phosphate dehydrogenase (G6PD) activity. SOD activity was assessed using a commercially available kit (Nanjing Jiancheng Bioengineering Institute, Cat#A001-3-1) based on the autooxidation of hydroxylamine, according to the manufacturer's instructions. The absorbance was measured at 450 nm using the EON microplate reader (Sartorius) G6PD activity was assessed using a commercially available kit (Shanghai Enzyme-linked Biotechnology Co. Ltd., Cat#MC8C5L). A total of 10 sample and 190 μl working solution were added to a 96-well plate, mixed and the absorbance at 340 nm (A1) was read using the EON microplate reader. Subsequently, the absorbance at 340 nm (A2) was read following incubation for 6 min at 37˚C. G6PD activity was calculated as follows: G6PD enzyme activity=1,286 x (A2-A1)/Cpr.

NADPH and NADP$^+$ content assay. NADPH and NADP$^+$ contents were measured using a coenzyme II (NADPH, NADP$^+$) content test kit (Nanjing Jiancheng Bioengineering Institute; cat#A115-1-1) according to the manufacturer's instructions (Nanjing Jiancheng Bioengineering Institute). Following centrifugation at 300 x g for 5 min at 4˚C in a 1.5 ml microcentrifuge tube, ~5x10^6 cells were collected, followed by the addition of 0.5 ml alkaline extraction buffer. The cells were sonicated on ice for 90 sec (2 sec on, 1 sec off) and boiled at 100˚C for 5 min. The cells were cooled on ice and centrifuged at 10,000 x g for 10 min at 4˚C. A total of 250 μl supernatant was neutralized with an equal volume of acidic extraction buffer and centrifuged again at 12,000 x g for 5 min at 4˚C. The protein concentration was measured using the BCA method. Absorbance was measured at 570 nm using a spectrophotometer, with double-distilled water as the blank control. The NADPH content was calculated as follows: NADPH content (nmol/mg protein)=0.8 x (ΔA-0.0259)/protein concentration.

For the measurement of the intracellular NADP$^+$ content, following centrifugation at 300 x g for 5 min at 4˚C, ~5x10^6 cells were collected into an EP tube followed by the addition of 0.5 ml acidic extraction buffer. The cells were sonicated and centrifuged as aforementioned. A total of 250 μl supernatant was transferred to a new EP tube, neutralized with an equal volume of alkaline extraction buffer and centrifuged again at 12,000 x g for 5 min at 4˚C. The protein concentration was

Table I. Primary antibodies.

Antibody	Supplier	Catalog No.
Nrf2	Zenbioscience	R380773
p-Nrf2	ABclonal	AP1133
G6PD	ABclonal	A1537
PGD	ABclonal	A0563
TKT	ABclonal	A6314
HO-1	ABclonal	A1346
HRP-conjugated goat anti-Rabbit IgG	ABclonal	AS014
HRP-conjugated Goat anti-Mouse IgG	ABclonal	AS003
β-actin	Sanjian Biotechnology	KM9006T

p-Nrf2, Phosphorylated nuclear factor erythroid 2-related factor 2; G6PD, glucose-6-phosphate dehydrogenase; PGD, 6-phosphogluconate dehydrogenase; TKT, transketolase; HO-1, heme oxygenase.

measured using the BCA method. The reaction and detection were carried out as aforementioned. The $NADP^+$ content was calculated as follows: $NADP^+$ content (nmol/mg protein)=5.1 x (ΔA-0.0144)/protein concentration.

Reverse transcription-quantitative (RT-q)PCR. Total RNA was extracted from approximately $5x10^6$ THP-1 cells using TRIzol reagent (Thermo Fisher Scientific, Inc.) and reverse-transcribed using a PrimeScript RT reagent kit (Takara Biotechnology Co., Ltd.) according to the manufacturer's instructions. qPCR was conducted on a Bio-Rad CFX96 system using the SYBR qPCR master mix (Toyobo Co., Ltd.) according to the manufacturer's protocol. Thermocycling conditions were as follows: Initial denaturation at 95˚C for 5 min; followed by 40 cycles of denaturation at 95˚C for 15 sec, annealing at 60˚C for 30 sec and extension at 72˚C for 30 sec. Analysis of relative gene expression data was performed via the 2-ΔΔCq method with β-actin as the endogenous control (15). RNA purity was assessed by measuring the A260/A280 ratio (1.8-2.0) using a NanoDrop 2000 spectrophotometer (Thermo Fisher Scientific) to confirm the absence of protein or solvent contamination. To ensure experimental reproducibility in downstream procedures, RNA concentrations were adjusted to 1 μg/μl using nuclease-free water (Thermo Fisher Scientific, Cat# AM9937). Primer-BLAST (v2.12.0; ncbi.nlm.nih.gov/tools/primer-blast/) was used to design the primers (Table II).

Nuclear and cytoplasmic protein extraction. To investigate xylitol-induced nuclear translocation of Nrf2 by western blotting, nuclear and cytoplasmic protein fractions were isolated using a Nuclear and Cytoplasmic Protein Extraction kit (Solarbio, Cat# EX1470). A total of ~$5x10^6$ treated THP-1 cells were washed with PBS and centrifuged at 500 x g for 2-3 min at 4˚C. Subsequently, the supernatant was aspirated, followed by the addition of 100 μl plasma protein extraction reagent (Solarbio, Cat# EX1470), mixing by blowing with a pipette and vortexing at 14 x g for 30 sec at 4˚C to obtain a single cell suspension. Following 10 min in an ice bath, the suspension was vortexed at 14 x g for 30 sec at 4˚C and centrifuged at 16,000 x g for 10 min at 4˚C. The supernatant containing cytoplasmic protein was stored at -80˚C for subsequent analysis. To isolate nuclear proteins, the remaining pellet was resuspended in 50 μl nuclear protein extraction reagent (Solarbio, Cat# EX1470) by pipette mixing (10x with a 200 μl tip) followed by vortexing at 14 x g for 30 sec at 4˚C. After 10 min incubation on ice, the suspension was vortexed (14 x g for 10 sec at 4˚C) and centrifuged at 16,000 x g for 10 min at 4˚C. The resulting nuclear protein supernatant was collected for downstream applications. The nuclear protein supernatant was either immediately processed or stored at -80˚C for future use, while the cytoplasmic fraction was preserved at -80˚C.

Statistical analysis. All data are presented as the mean ± SD of ≥3 experiments performed in parallel. Statistical analyses were performed using one-way analysis of variance followed by Bonferroni's multiple comparison test using GraphPad Prism 10 software (Dotmatics, Inc.). $P<0.05$ was considered to indicate a statistically significant difference.

Results

PPP is a Key Metabolic Signature in Atherosclerosis. Gene differential expression analysis was performed for the control and AS model groups, followed by GO and KEGG analyses. GO enrichment analysis revealed that the differentially expressed genes were enriched in 'endosome membrane' and 'melanosome', molecular functions, such as 'immune receptor activity', 'oxidoreductase activity' and 'sterol binding' molecules, and 'pentose-phosphate pathway' (Fig. 2A). KEGG analysis (Fig. 2B) demonstrated that several pathways, including 'pentose-phosphate pathway', were enriched. To explore the expression of the PPP in the AS model group, GSEA was performed out to examine the differences in expression between the control and AS model groups (Fig. 2C). Analysis revealed that the PPP had enrichment score (ES) >0.4, indicating significant upregulation in the model group, suggesting that AS was positively associated with the PPP.

Optimal concentration of xylitol. Based on the CCK-8 assay, the optimal concentration of xylitol was determined. Xylitol significantly affected THP-1 cell viability in a concentration-dependent manner (Fig. 3A) at ≥150 mM. Cell viability was not notably affected by xylitol treatment at low concentrations (0-100 mM; Fig. 3B). However, at concentrations ≥200 mM, the viability of the cells decreased and apoptosis and necrosis increased. Therefore, 100 mM xylitol was used as the highest concentration in subsequent experiments.

Xylitol inhibits oxidative stress in THP-1 cells induced by high levels of LDL. Levels of oxidative stress were assessed by detecting the MDA content. MDA levels were unaltered across experimental groups exposed to xylitol concentrations ranging from 100 μM to 10 mM, demonstrating no substantial assay interference from the polyol across the tested concentration

Table II. Reverse transcription-quantitative PCR primers.

Gene	Forward primer, 5' to 3'	Reverse primer (5' to 3')
SOD1	ACAAAGATGGTGTGGCCGAT	AACGACTTCCAGCGTTTCCT
SOD2	GCACTAGCAGCATGTTGAGC	CCGTTAGGGCTGAGGTTTGT
G6PD	CGACGACGAAGCGCAGA	TGAAGGTGTTTTCGGGCAGA
PGD	GCTCTTCGGTTCTGCTCTGT	TCTCGGCACCGTCTCAATTT
TKT	ACTTCGACAAGGCCAGCTAC	GCCCAGGCGATTGATGTCTA
HO-1	AAGATTGCCCAGAAAGCCCTGGAC	AACTGTCGCCACCAGAAAGCTGAG
Nrf2	CAGTCAGCGACGGAAAGAGTA	CTGGGAGTAGTTGGCAGATCC
NQO1	GCTGGTTTGAGCGAGTGTTC	CTGCCTTCTTACTCCGGAAGG
KEAP1	CCTCTGGCCGGGTAATAGG	CCCCTCCCAGGTATCCAAGA
Nox1	TAAAGGCTCACAGACCCTGC	AGCCTAACCAAACAACCAGA
Nox2	TGTGTGAATGCCCGAGTCAA	GCCCACGTACAATTCGTTCAG
Nox4	CAGATGTTGGGGCTAGGATTG	GAGTGTTCGGCACATGGGTA
β-actin	CTTCGCGGGCGACGAT	CCACATAGGAATCCTTCTGACC

SOD, superoxide dismutase; G6PD, glucose-6-phosphate dehydrogenase; PGD, 6-phosphogluconate dehydrogenase; TKT, transketolase; HO-1, heme oxygenase; NQO1, NAD(P)H quinone dehydrogenase 1; KEAP1, kelch-like ECH-associated protein 1; NOX, NADPH oxidase.

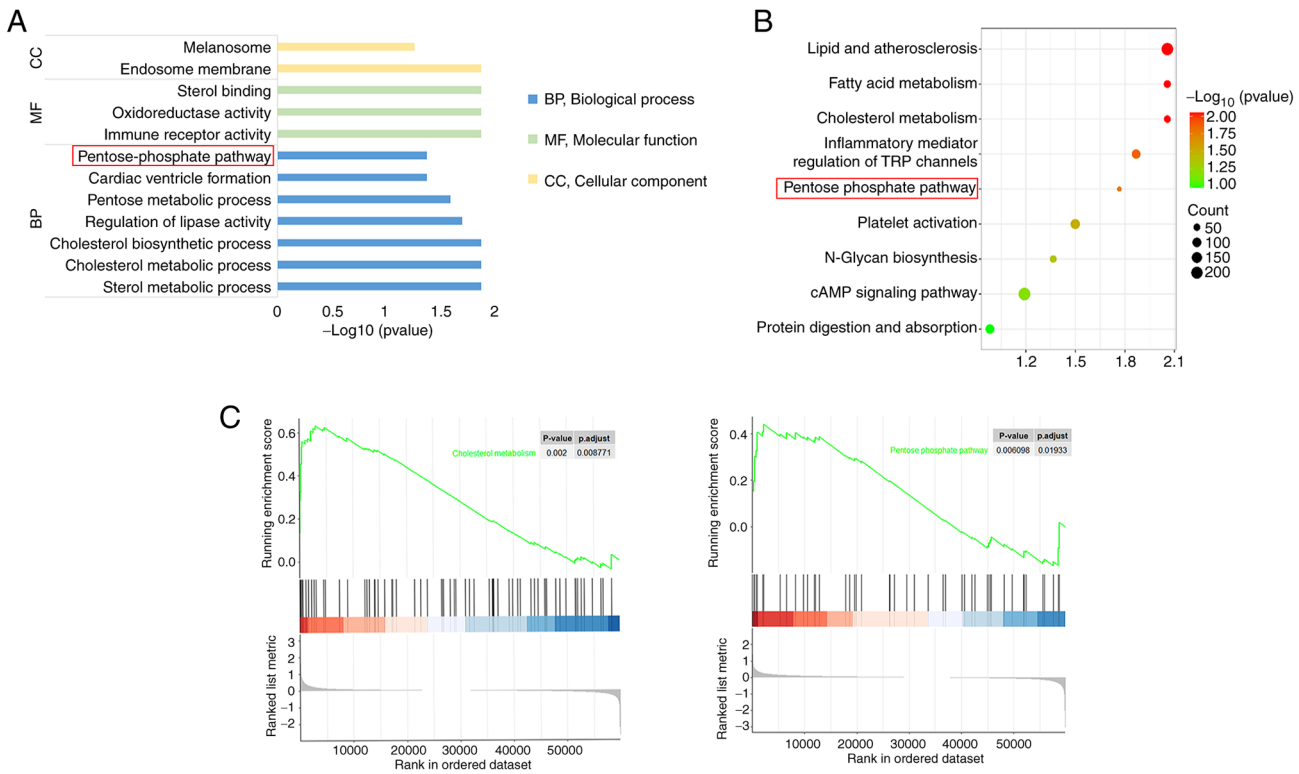

Figure 2. Bioinformatics analysis of pathway changes in atherosclerosis. (A) Gene Ontology and (B) Kyoto Encyclopedia of Genes and Genomes analyses. (C) Representative pathways determined using Gene Set Enrichment Analysis.

spectrum (Fig. S1). Compared with the control, the MDA levels were significantly increased in the LDL-treated group. Conversely, co-incubation with LDL and xylitol led to a significant decrease in MDA levels compared with the LDL group (Fig. 4A). DCFH-DA probe to detect levels of ROS demonstrated increased relative fluorescence quantification in the native LDL group compared with the control, suggesting elevated levels of ROS (Fig. 4B and C). However, following the addition of xylitol, the relative fluorescence quantification decreased, accompanied by a leftward peak shift relative to the LDL group, indicating decreased levels of ROS in the THP-1 cells. GSH levels, a key antioxidant for cellular regulation (16), were increased in the LDL + xylitol compared with the LDL-only group (Fig. 4D). These findings suggested that xylitol mitigated oxidative stress induced by high LDL levels in THP-1 cells.

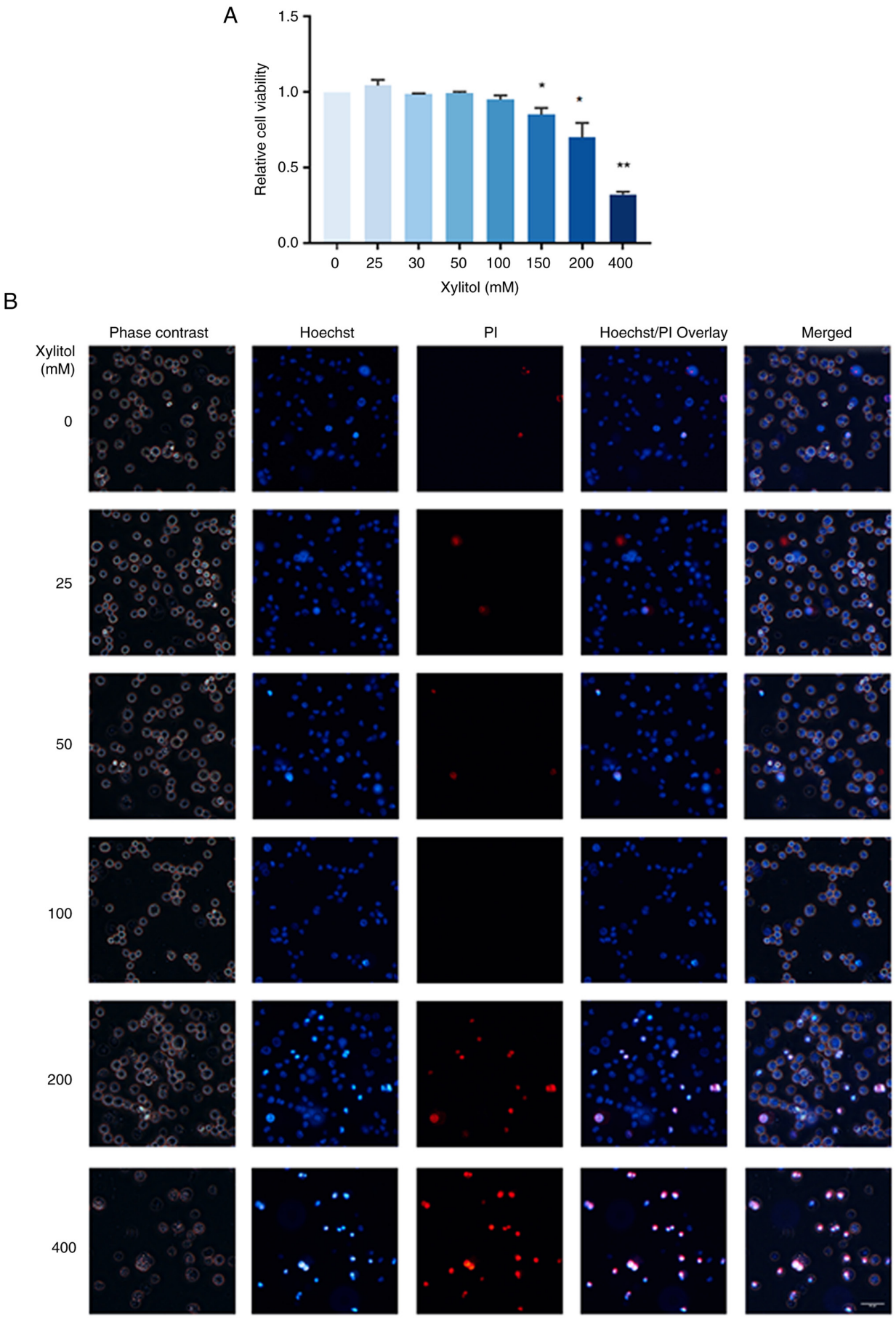

Figure 3. Effect of xylitol on THP-1 cells. (A) Viability of THP-1 cells treated with xylitol was determined using Cell Counting Kit-8 assay. Following 24 h of xylitol treatment, the viability of THP-1 cells significantly decreased at a concentration of 150 mM. (B) Representative Hoechst 33342/PI staining. *P<0.05, **P<0.01 vs. control.

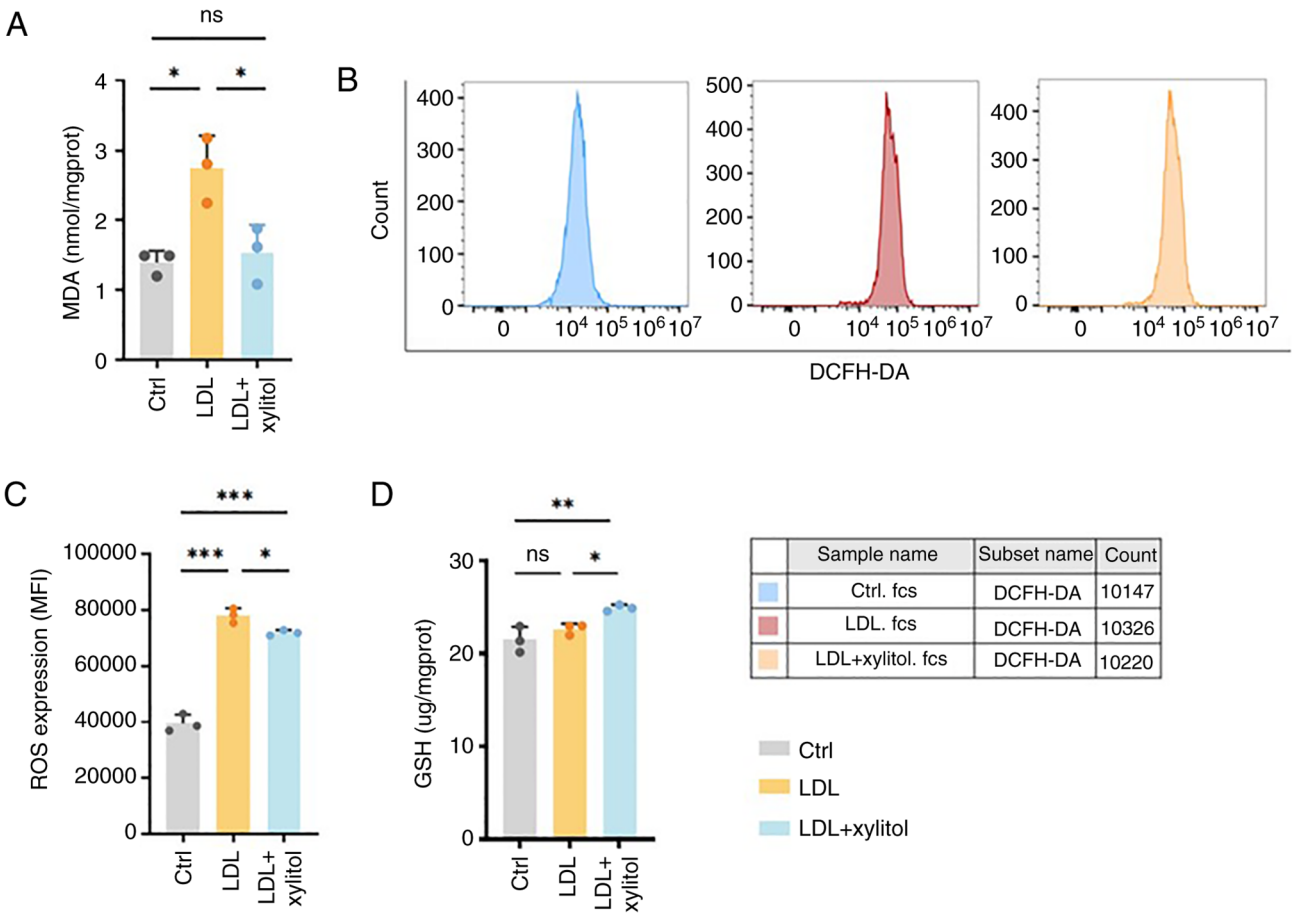

Figure 4. Effect of xylitol on LDL oxidation in THP-1 cells. (A) MDA content. (B) Flow cytometry. (C) Quantified relative fluorescence. (D) GSH levels. *P<0.05, **P<0.01, ***P<0.001. LDL, low-density lipoprotein; MDA, malondialdehyde; GSH, glutathione; ROS, reactive oxygen species; DCFH-DA, dichlorodihydrofluorescein diacetate; MFI, mean fluorescence intensity; ns, not significant; ctrl, control; prot, protein.

Xylitol decreases intracellular LDL oxidation in THP-1 cells through the NADPH and SOD systems. Intracellular SOD activity increased in the LDL-only compared with the control group, and this elevation was further amplified by xylitol co-treatment (Fig. 5A). There was no significant alteration in SOD1 mRNA expression in the LDL + xylitol co-incubation group compared with that in the LDL group. However, SOD2 mRNA expression was significantly upregulated (Fig. 5B). Compared to the control group, LDL treatment significantly elevated oxidative stress markers NOX1 and NOX2, while NOX4 showed no significant alteration (Fig. 5C). These increased levels indicated an increase in oxidative stress. Following the addition of xylitol, the mRNA levels of NOX1 and NOX2 decreased significantly, whereas the mRNA expression of NOX4 was not significantly altered.

Xylitol decreases intracellular LDL oxidation in THP-1 cells by activating the PPP. Compared with the LDL group, xylitol resulted in the upregulation of G6PD protein and mRNA (Fig. 6A-C). G6PD/TKT expression after LDL treatment was not significantly altered compared with control. Furthermore, G6PD enzyme activity significantly increased (Fig. 6D). 6-phosphogluconate dehydrogenase (PGD) is the second enzyme in the oxidative phase of the PPP (17). Protein and RNA levels of PGD significantly increased, indicating that xylitol significantly promoted the upregulation of molecules associated with the oxidative phase of PPP (Fig. 6A-C). Transketolase (TKT) is a thiamine diphosphate-dependent enzyme that catalyzes reversible reactions in the non-oxidative branch of PPP and serves as a bridge between PPP and glycolysis (18). TKT catalyzes the conversion of xylulose-5-phosphate (X5P) and ribulose-5-phosphate, which are key enzymes for the participation of the xylitol metabolite X5P in the PPP (19). A significant increase in both the protein and mRNA levels of TKT was observed following the addition of xylitol compared with the model group, suggesting that xylitol promoted expression of molecules associated with the non-oxidative phase of the PPP, but TKT expression showed no significant difference between the LDL-treated and control groups (Fig. 6A-C). NADPH, a key product of the PPP, and its derivative glutathione disulfide, which is reduced to glutathione (GSH) by glutathione reductase, serve key roles in cellular antioxidant defense (13). Xylitol increased NADPH and $NADP^+$ levels compared with the LDL model group (Fig. 6E). As shown in Fig. 6E, the NADPH/$NADP^+$ ratio was significantly decreased in the LDL-treated group compared with the control, whereas xylitol supplementation restored this ratio to levels exceeding those of the LDL-only group. These results suggested that the addition of xylitol promoted the upregulation of the PPP and the expression of key molecules in both the oxidative and non-oxidative phases at both the protein and mRNA levels, which promoted the NADPH/$NADP^+$ ratio and attenuated the oxidation of LDL in THP-1 cells.

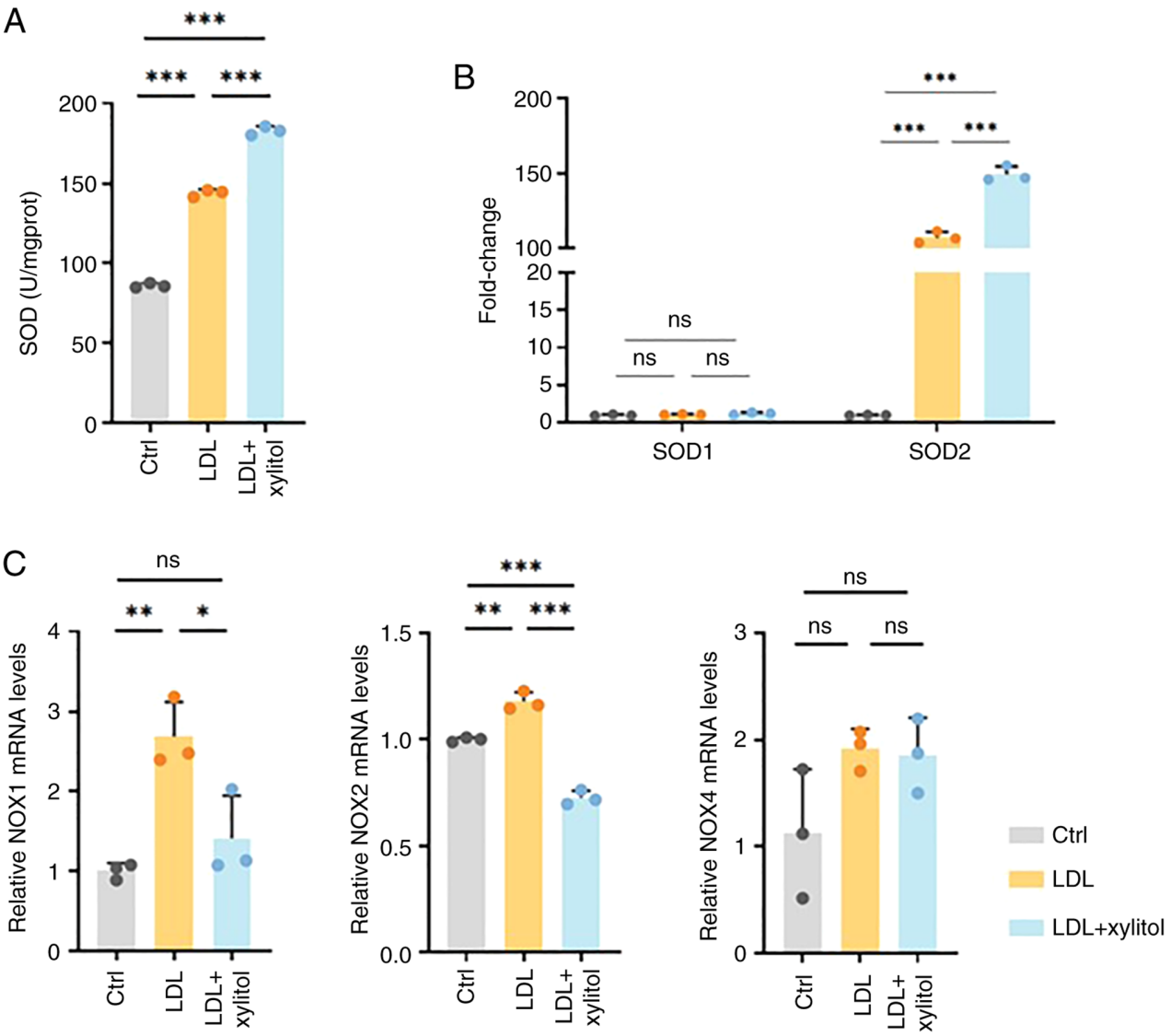

Figure 5. Effect of xylitol on native LDL oxidation in THP-1 cells. (A) SOD content. Relative mRNA expression of (B) SOD1 and SOD2 and (C) NOX1, NOX2 and NOX4. *P<0.05, **P<0.01, ***P<0.001. LDL, low-density lipoprotein; SOD, superoxide dismutase; NOX, NADPH oxidase; ctrl, control; ns, not significant; prot, protein.

Xylitol promotes Nrf2/heme oxygenase-1 (HO-1) signaling to reduce LDL oxidation in THP-1 cells. As Nrf2 is a transcription factor that regulates the PPP and redox homeostasis in cells and G6PD is a target gene of Nrf2 (20), the present study investigated whether Nrf2 regulates LDL oxidation in THP-1 cells. Xylitol significantly increased the mRNA expression of Nrf2 compared with that in the LDL group. The mRNA levels of HO-1 (the target gene of Nrf2) exhibited a similar trend (Fig. 7A). Xylitol significantly increased the HO-1 protein levels compared with the LDL group (Fig. 7B). Although LDL and xylitol co-treatment elevated Nrf2 mRNA expression compared with LDL alone, total Nrf2 protein levels showed no significant difference between the two groups (Fig. 7C).

Xylitol decreases oxidative stress by promoting phosphorylation and nuclear isomerization of Nrf2. The phosphorylation of Nrf2 affects the charge properties that modulate DNA-binding activity (21). As there was no difference in the expression of Nrf2 protein in the LDL and the LDL and xylitol co-incubation group, but the Nrf2 mRNA levels increased and there were changes in expression of target genes of Nrf2, the protein levels of phosphorylated (p-)Nrf2 was examined. Xylitol significantly increased the p-Nrf2 protein levels compared with the LDL group (Fig. 8A and B). Nrf2 increases the transcription of antioxidant proteins by binding antioxidant response elements, which are translocated to the nucleus to exert their effects (22). Therefore, the present study investigated whether xylitol promoted the cytosolic translocation of Nrf2. However, compared with the LDL group, the expression level of Nrf2 was increased in the cytoplasm following the addition of xylitol and expression of Nrf2 was decreased in THP-1 cells, suggesting that xylitol altered nucleocytoplasmic shuttling rather than canonical activation of Nrf2 (Fig. 8C and D).

Discussion

Xylitol attenuates LDL oxidative modification in THP-1 macrophages via Nrf2-dependent transcriptional regulation

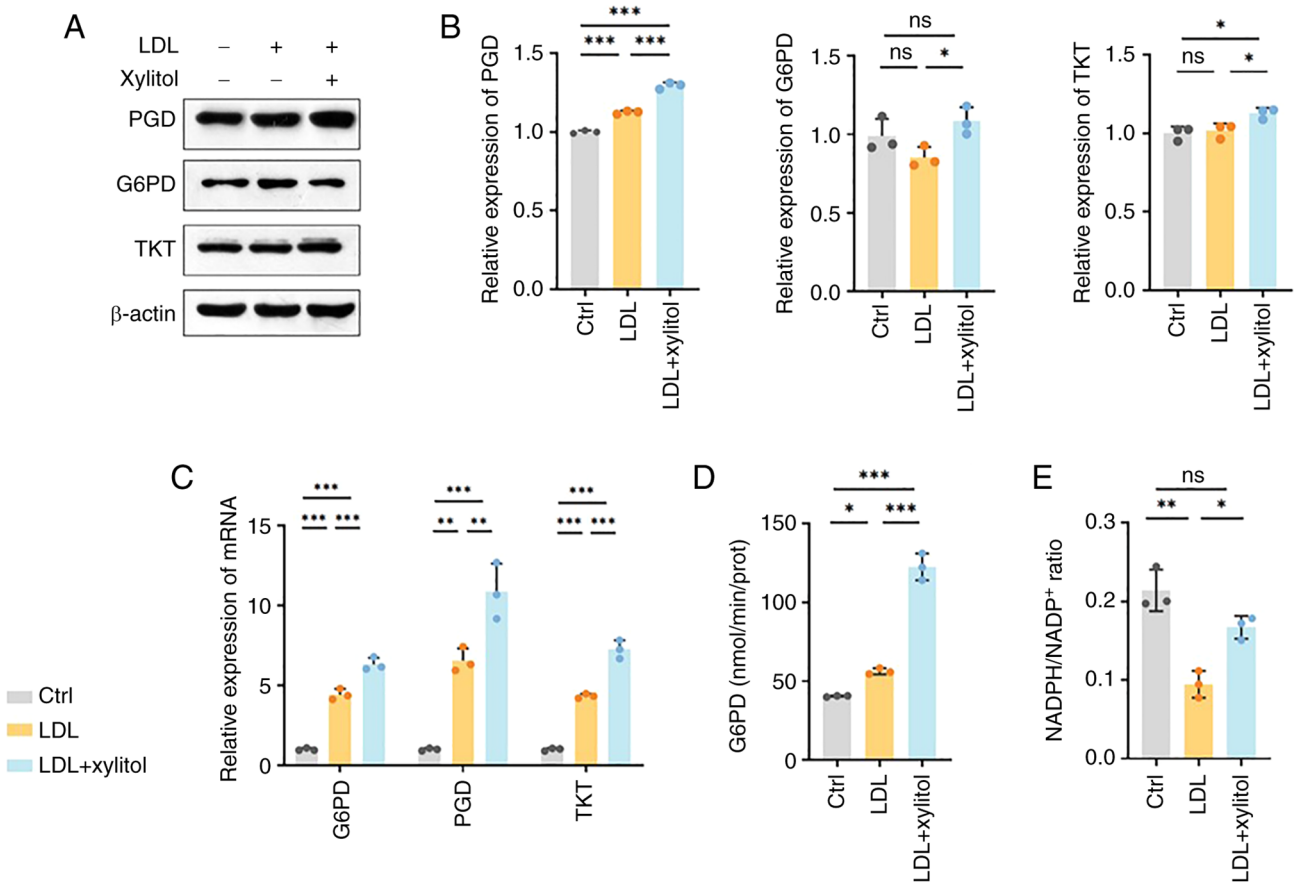

Figure 6. Xylitol activates the pentose phosphate pathway. (A) Representative western blot bands of (B) PGD, G6PD and TKT. (C) mRNA expression levels of G6PD, PGD and TKT. (D) Enzyme activity of G6PD. (E) NADPH/NADP+ ratio. *P<0.05, **P<0.01, ***P<0.001. PGD, phosphogluconate dehydrogenase; G6PD, glucose-6-phosphate dehydrogenase; TKT, transketolase; LDL, low-density lipoprotein; ctrl, control; ns, not significant; prot, protein.

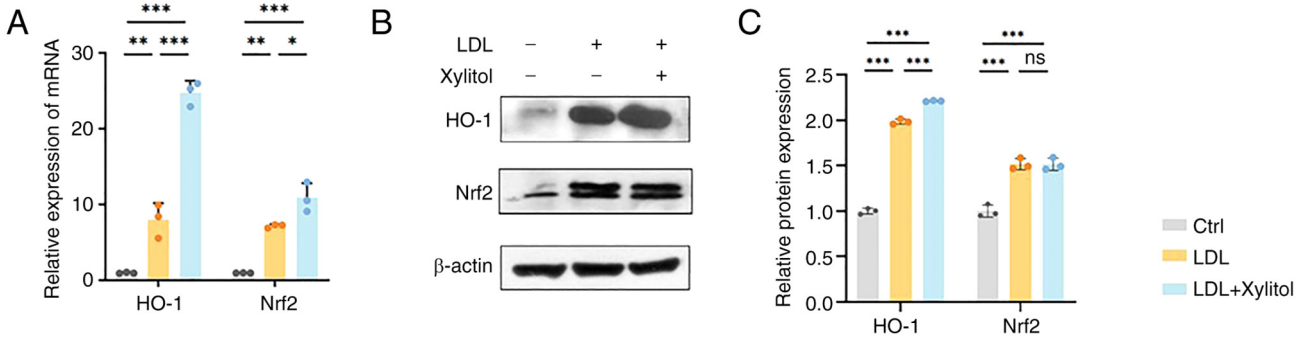

Figure 7. Xylitol promotes the activation of the Nrf2/HO-1 axis. (A) mRNA expression levels of HO-1 and Nrf2. (B) Representative western blot bands of (C) HO-1 and Nrf2. *P<0.05, **P<0.01, ***P<0.001. LDL, low-density lipoprotein; HO-1, heme oxygenase-1; ctrl, control; ns, not significant.

of the pentose phosphate pathway, resulting in increased NADPH/NADP+ ratio, activation of the Nrf2/HO-1 antioxidant axis, and consequent reduction of intracellular ROS (Fig. 9).

Xylitol is metabolized to D-xylulose 5-phosphate ($C_5H_{11}O_8P$), an essential component of the PPP (23). Xylitol undergoes polyol metabolism, and its products are involved in the PPP. Increased NADPH levels in the PPP decrease oxidative stress. According to Chukwuma and Islam (11), xylitol exerts antioxidant effects and ameliorates oxidative stress in a rat model of diabetes. Therefore, the present study investigated whether xylitol has similar effects in an *in vitro* AS model and whether it influences cellular oxidation levels via the PPP.

Bioinformatics analysis identified changes in the PPP in AS. Park *et al* (24) treated THP-1 cells with xylitol for 24 or 48 h and found that concentrations ≥197 mmol/l caused a decrease in cell viability (24), which was consistent with the results of the present study. Dose-optimization experiments demonstrated that 100 mM xylitol (the highest concentration tested) achieved maximal PPP modulation without cytotoxicity. This concentration was therefore selected for all subsequent experiments.

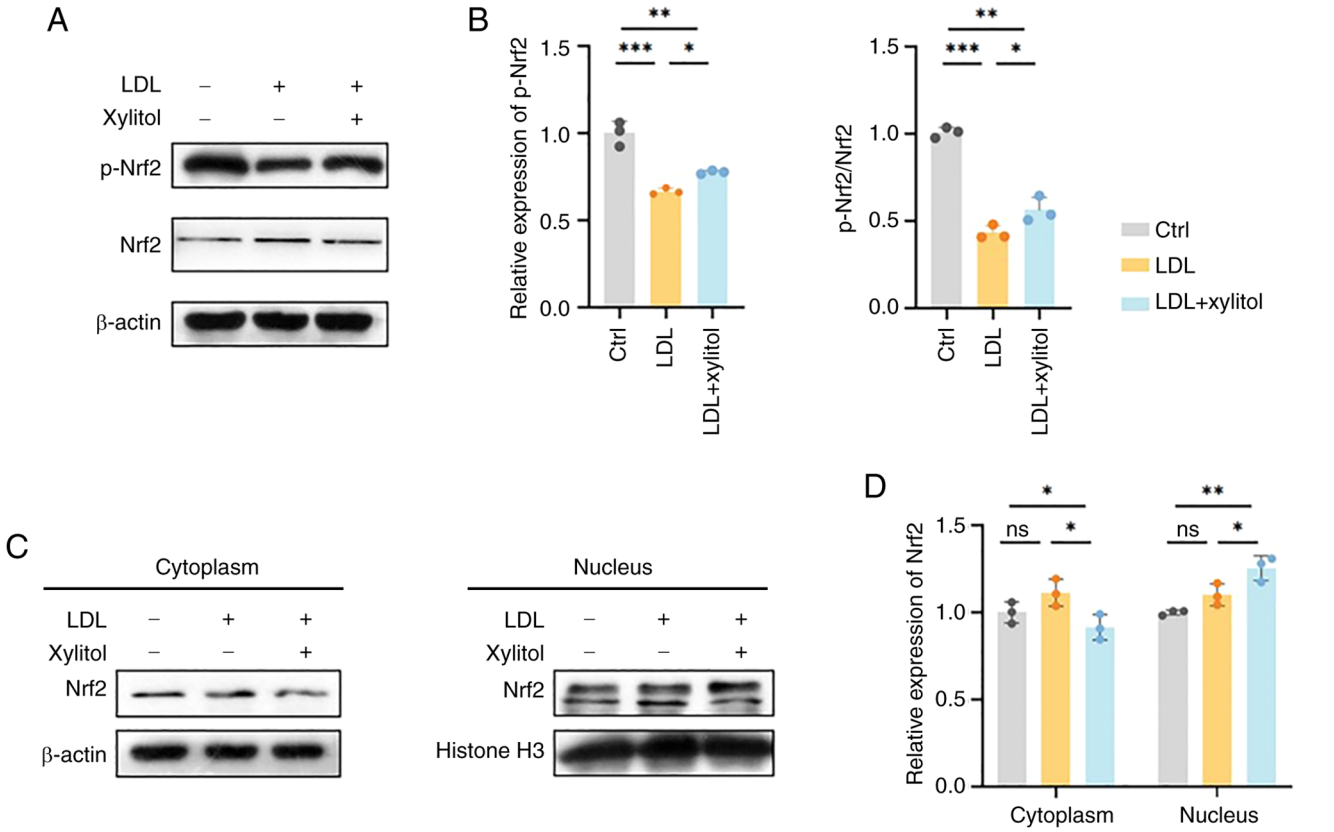

Figure 8. Xylitol promotes Nrf2 phosphorylation and nuclear translocation. (A) Representative western blot bands of (B) p-Nrf2. (C) Representative western blot bands of (D) Nrf2 in cytoplasm and nucleus. *P<0.05, **P<0.01, ***P<0.001. LDL, low-density lipoprotein; p-, phosphorylated; ctrl, control; ns, not significant.

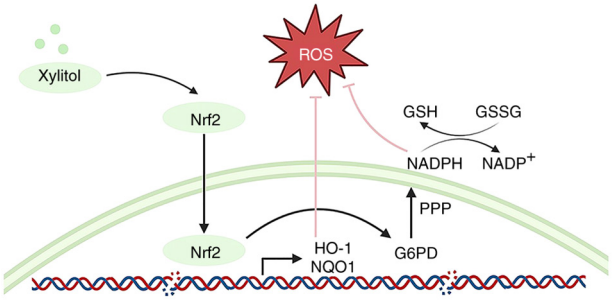

Figure 9. Xylitol elevates the NADPH/NADP^{+} ratio via Nrf2 transcription factor-mediated modulation of the PPP, activates the Nrf2/HO-1 axis to lower ROS levels and reduces LDL oxidative modification in THP-1 cells. LDL, low-density lipoprotein; ROS, reactive oxygen species; HO-1, heme oxygenase 1; NQO1, NAD(P)H quinone dehydrogenase 1; G6PD, glucose-6-phosphate dehydrogenase; GSH, Glutathione disulfide; PPP, pentose phosphate pathway; GSSG, Glutathione disulfide.

Oxidative stress is implicated in the pathogenesis of AS and there is increasing evidence to indicate that it serves a key role in its development (25,26). MDA is a primary end product of membrane lipid peroxidation during cellular oxidative stress (27). The present study revealed that MDA levels in THP-1 cells increased following LDL stimulation, while co-incubation with xylitol significantly decreased MDA levels, indicating that xylitol alleviated LDL-induced cellular oxidative damage. Xylitol is a five-carbon sugar alcohol with relatively weak reducing activity. Although xylitol exhibits reducing properties, its chemical structure results in low reactivity with thiobarbituric acid, the reagent used in the MDA assay, leading to minimal interference (10). The intracellular GSH levels in THP-1 cells increased in the LDL + xylitol group compared with the LDL model group. In a study by Abulizi *et al* (28) on serum from a rat model of AS, the GSH levels decreased in the AS model group compared with the control. By contrast, in the present study, in the LDL model group, intracellular GSH levels did not decrease, potentially as it was in the early compensatory state of regulating oxidation levels. ROS levels in THP-1 cells were measured. Following LDL stimulation, the peak of the fluorescence signal appeared to shift to the right and the oxidation level increased. Following the addition of xylitol, the peaks shifted to the left compared with those of the LDL group, indicating that the addition of xylitol reduced ROS levels and oxidation of LDL in THP-1 cells. Future studies should use electron spin resonance to enable real-time detection of ROS to determine the underlying molecular mechanisms.

NOXs are specialized enzymes responsible for producing ROS, with their activation resulting in the formation of superoxide (29). To date, seven NOX isoforms (NOX1, NOX2, NOX3, NOX4, NOX5, Duox1 and Duox2) have been identified. These enzymes participate in cellular processes such as signal transduction in cellular stress responses, with isoform expression being cell-specific and each NOX

exhibiting unique physiological and pathological roles (30). Studies have shown that the expression of NOX1 in human aortic smooth muscle cells increases following stimulation with oxidized LDL, which increases the intracellular oxidation and participates in the occurrence of AS (31,32). Moreover, NOX2 is a primary source of ROS and its increased expression is associated with plaque development (33). NOX2-mediated oxidative stress homeostasis is key in AS (34). Therefore, the present study examined the mRNA expression of NOX1, NOX2 and NOX4 in the NADPH oxidase system and found that xylitol decreased the mRNA levels of NOX1 and NOX2. SOD, a key endogenous antioxidant enzyme, has a key role in cardiovascular diseases. SOD2 is associated with development of AS, and SOD2 deficiency under hyperlipidemic conditions leads to increased mitochondrial oxidative stress in mice, which induces AS plaque destabilization (35). In the present study, co-treatment of xylitol with LDL resulted in a significant increase in SOD enzyme activity and an increase in SOD2 mRNA levels compared with the LDL group. The present study demonstrated that xylitol reduced LDL oxidation in THP-1 cells by increasing the activity and subunit mRNA levels of the antioxidant SOD system and decreased the subunit mRNA levels of NOX system.

NADPH is a key intracellular antioxidant required for the maintenance of redox homeostasis by the GSH system and other ROS scavengers, and the primary source of cytoplasmic NADPH is the PPP (36). The present study indicated that xylitol upregulated the protein and mRNA levels of key regulatory enzymes, G6PD and PGD, in the PPP. Furthermore, an increase in content of G6PD was observed. G6PD, the first rate-limiting enzyme in the oxidative branch of the PPP, serves a key role in generating NADPH and regenerating GSH, thereby decreasing ROS levels (37). Reduced NADPH levels in patients with G6PD deficiency leads to impaired GSH regeneration and oxidative damage in red blood cells (12). The elevation of G6PD and PGD levels suggests enhanced oxidative pathways in the PPP. Additionally, NADPH/$NADP^+$ ratio increased significantly. Subsequently, the present study investigated the protein and mRNA levels of TKT, a non-oxidative pathway enzyme in PPP, which exhibited elevated levels. Collectively, these findings indicated that xylitol activates the PPP by increasing the expression levels of key enzymes, thereby increasing the NADPH/$NADP^+$ ratio and ameliorating high LDL-induced oxidative stress in THP-1 cells.

Nrf2 is a key transcription factor that regulates oxidative stress (38). Under physiological conditions, Nrf2 undergoes ubiquitination and degradation, mediated by its specific inhibitor, kelch-like ECH-associated protein 1 (KEAP1). However, under stress, Nrf2 dissociates from KEAP1, translocates from the cytoplasm to the nucleus and binds antioxidant response elements, thereby activating the transcription of antioxidant defense genes such as HO-1, leading to the rapid clearance of ROS and the alleviation of oxidative damage (39). Furthermore, Nrf2 regulates GSH synthesis (40). Nrf2 directly activates G6PD by binding antioxidant response elements in the G6PD promoter (41). HO-1 serves as an Nrf2 regulatory gene; the Nrf2/HO-1 system has a key role in AS and is a notable defense mechanism against cardiovascular disease (42). In a previous study, increased Nrf2/HO-1 signaling was observed in monocyte-derived macrophages within patients with cardiovascular disease when compared with healthy individuals (43). The present study demonstrated that following xylitol supplementation, the mRNA levels of Nrf2 and its target gene, HO-1, increased. However, while the expression of HO-1 increased at the protein level, there was no change in the total Nrf2 protein levels. Therefore, the present study examined the expression of p-Nrf2 and observed an increase at the protein level. Further investigation revealed an increase in nuclear Nrf2 and a decrease in cytoplasmic Nrf2 expression following xylitol supplementation compared with the LDL model group, with no change in the total Nrf2 expression. These results suggested that xylitol decreased LDL-induced oxidative stress in THP-1 cells by promoting the activation of Nrf2/HO-1 signaling and facilitating Nrf2 phosphorylation and nuclear translocation.

In conclusion, the present study demonstrated that xylitol significantly decreased oxidative stress induced by high levels of LDL in THP-1 cells, as well as ROS and MDA levels and NOX family enzyme expression, and increased antioxidant enzyme SOD activity and expression and GSH levels. This was achieved by regulating the PPP via the Nrf2 transcription factor to increase the NADPH/$NADP^+$ ratio and activate the Nrf2/HO-1 axis to decrease oxidative modification of LDL in THP-1 cells.

Acknowledgements

Not applicable.

Funding

The present study was supported by Natural Science Foundation of Hubei Province, China (grant no. 2024AFC016).

Availability of data and materials

The data generated in the present study may be requested from the corresponding author.

Authors' contributions

JW and YL designed the study. ZH, AL, MS, RH, RY, WW and ZH performed experiments and analyzed data. ZH wrote the manuscript. All authors have read and approved the final manuscript. ZH and AL confirm the authenticity of all the raw data.

Ethics approval and consent to participate

Not applicable.

Patient consent for publication

Not applicable.

Competing interests

The authors declare that they have no competing interests.

References

1. Wang B, Tang X, Yao L, Wang Y, Chen Z, Li M, Wu N, Wu D, Dai X, Jiang H and Ai D: Disruption of USP9X in macrophages promotes foam cell formation and atherosclerosis. J Clin Invest 132: e154217, 2022.
2. Martin SS, Aday AW, Allen NB, Almarzooq ZI, Anderson CAM, Arora P, Avery CL, Baker-Smith CM, Bansal N, Beaton AZ, *et al*: 2025 Heart disease and stroke statistics: A report of US and global data from the American heart association. Circulation 151: e41-e660, 2025.
3. Kong P, Cui ZY, Huang XF, Zhang DD, Guo RJ and Han M: Inflammation and atherosclerosis: Signaling pathways and therapeutic intervention. Signal Transduct Target Ther 7: 131, 2022.
4. Raitakari O, Pahkala K and Magnussen CG: Prevention of atherosclerosis from childhood. Nat Rev Cardiol 19: 543-554, 2022.
5. Ference BA, Ginsberg HN, Graham I, Ray KK, Packard CJ, Bruckert E, Hegele RA, Krauss RM, Raal FJ, Schunkert H, *et al*: Low-density lipoproteins cause atherosclerotic cardiovascular disease. 1. Evidence from genetic, epidemiologic, and clinical studies. A consensus statement from the European atherosclerosis society consensus panel. Eur Heart J 38: 2459-2472, 2017.
6. Kianmehr A, Qujeq D, Bagheri A and Mahrooz A: Oxidized LDL-regulated microRNAs for evaluating vascular endothelial function: Molecular mechanisms and potential biomarker roles in atherosclerosis. Crit Rev Clin Lab Sci 59: 40-53, 2022.
7. Yan R, Zhang X, Xu W, Li J, Sun Y, Cui S, Xu R, Li W, Jiao L and Wang T: ROS-induced endothelial dysfunction in the pathogenesis of atherosclerosis. Aging Dis 16: 250-268, 2024 (Epub ahead of print).
8. Prasad K and Mishra M: Mechanism of hypercholesterolemia-induced atherosclerosis. Rev Cardiovasc Med 23: 212, 2022.
9. Gasmi Benahmed A, Gasmi A, Arshad M, Shanaida M, Lysiuk R, Peana M, Pshyk-Titko I, Adamiv S, Shanaida Y and Bjørklund G: Health benefits of xylitol. Appl Microbiol Biotechnol 104: 7225-7237, 2020.
10. Msomi NZ, Erukainure OL, Salau VF, Olofinsan KA and Islam MS: Xylitol improves antioxidant, purinergic and cholinergic dysfunction, and lipid metabolic homeostasis in hepatic injury in type 2 diabetic rats. J Food Biochem 46: e14040, 2022.
11. Chukwuma CI and Islam S: Xylitol improves anti-oxidative defense system in serum, liver, heart, kidney and pancreas of normal and type 2 diabetes model of rats. Acta Pol Pharm 74: 817-826, 2017.
12. TeSlaa T, Ralser M, Fan J and Rabinowitz JD: The pentose phosphate pathway in health and disease. Nat Metab 5: 1275-1289, 2023.
13. Hayes JD, Dinkova-Kostova AT and Tew KD: Oxidative stress in cancer. Cancer Cell 38: 167-197, 2020.
14. Koutsaliaris IK, Moschonas IC, Pechlivani LM, Tsouka AN and Tselepis AD: Inflammation, oxidative stress, vascular aging and atherosclerotic ischemic stroke. Curr Med Chem 29: 5496-5509, 2022.
15. Livak KJ and Schmittgen TD: Analysis of relative gene expression data using real-time quantitative PCR and the 2(-Delta Delta C(T)) method. Methods 25: 402-408, 2001.
16. Liu Y, Liu S, Tomar A, Yen FS, Unlu G, Ropek N, Weber RA, Wang Y, Khan A, Gad M, *et al*: Autoregulatory control of mitochondrial glutathione homeostasis. Science 382: 820-828, 2023.
17. Patra KC and Hay N: The pentose phosphate pathway and cancer. Trends Biochem Sci 39: 347-354, 2014.
18. Stincone A, Prigione A, Cramer T, Wamelink MM, Campbell K, Cheung E, Olin-Sandoval V, Grüning NM, Krüger A, Tauqeer Alam M, *et al*: The return of metabolism: biochemistry and physiology of the pentose phosphate pathway. Biol Rev Camb Philos Soc 90: 927-963, 2015.
19. Fullam E, Pojer F, Bergfors T, Jones TA and Cole ST: Structure and function of the transketolase from Mycobacterium tuberculosis and comparison with the human enzyme. Open Biol 2: 110026, 2012.
20. Smith MJ, Yang F, Griffiths A, Morrell A, Chapple SJ, Siow RCM, Stewart T, Maret W and Mann GE: Redox and metal profiles in human coronary endothelial and smooth muscle cells under hyperoxia, physiological normoxia and hypoxia: Effects of NRF2 signaling on intracellular zinc. Redox Biol 62: 102712, 2023.
21. Huang HC, Nguyen T and Pickett CB: Phosphorylation of Nrf2 at Ser-40 by protein kinase C regulates antioxidant response element-mediated transcription. J Biol Chem 277: 42769-42774, 2002.
22. Jiang X, Yu M, Wang WK, Zhu LY, Wang X, Jin HC and Feng LF: The regulation and function of Nrf2 signaling in ferroptosis-activated cancer therapy. Acta Pharmacol Sin 45: 2229-2240, 2024.
23. Vincent MF, Van den Berghe G and Hers HG: D-xylulose-induced depletion of ATP and Pi in isolated rat hepatocytes. FASEB J 3: 1855-1861, 1989.
24. Park E, Na HS, Kim SM, Wallet S, Cha S and Chung J: Xylitol, an anticaries agent, exhibits potent inhibition of inflammatory responses in human THP-1-derived macrophages infected with Porphyromonas gingivalis. J Periodontol 85: e212-e223, 2014.
25. Batty M, Bennett MR and Yu E: The role of oxidative stress in atherosclerosis. Cells 11: 3843, 2022.
26. Violi F, Pignatelli P and Valeriani E: Oxidative stress and atherosclerosis: Basic and clinical open issues. Kardiol Pol 82: 689-691, 2024.
27. Cordiano R, Di Gioacchino M, Mangifesta R, Panzera C, Gangemi S and Minciullo PL: Malondialdehyde as a potential oxidative stress marker for allergy-oriented diseases: An update. Molecules 28: 5979, 2023.
28. Abulizi A, Simayi J, Nuermaimaiti M, Han M, Hailati S, Talihati Z, Maihemuti N, Nuer M, Khan N, Abudurousuli K, *et al*: Quince extract resists atherosclerosis in rats by down-regulating the EGFR/PI3K/Akt/GSK-3β pathway. Biomed Pharmacother 160: 114330, 2023.
29. Xu Q, Choksi S, Qu J, Jang J, Choe M, Banfi B, Engelhardt JF and Liu ZG: NADPH oxidases are essential for macrophage differentiation. J Biol Chem 291: 20030-20041, 2016.
30. Jiang F, Zhang Y and Dusting GJ: NADPH oxidase-mediated redox signaling: Roles in cellular stress response, stress tolerance, and tissue repair. Pharmacol Rev 63: 218-242, 2011.
31. Yin CC and Huang KT: H2O2 but not O2-elevated by oxidized LDL enhances human aortic smooth muscle cell proliferation. J Biomed Sci 14: 245-254, 2007.
32. Gimenez M, Schickling BM, Lopes LR and Miller FJ Jr: Nox1 in cardiovascular diseases: Regulation and pathophysiology. Clin Sci (Lond) 130: 151-165, 2016.
33. Vermot A, Petit-Härtlein I, Smith SME and Fieschi F: NADPH oxidases (NOX): An overview from discovery, molecular mechanisms to physiology and pathology. Antioxidants (Basel) 10: 890, 2021.
34. Wang Y, Liu XY, Wang Y, Zhao WX, Li FD, Guo PR, Fan Q and Wu XF: NOX2 inhibition stabilizes vulnerable plaques by enhancing macrophage efferocytosis via MertK/PI3K/AKT pathway. Redox Biol 64: 102763, 2023.
35. Vendrov AE, Stevenson MD, Alahari S, Pan H, Wickline SA, Madamanchi NR and Runge MS: Attenuated superoxide dismutase 2 activity induces atherosclerotic plaque instability during aging in hyperlipidemic mice. J Am Heart Assoc 6: e006775, 2017.
36. Masi A, Mach RL and Mach-Aigner AR: The pentose phosphate pathway in industrially relevant fungi: Crucial insights for bioprocessing. Appl Microbiol Biotechnol 105: 4017-4031, 2021.
37. Chen PH, Tjong WY, Yang HC, Liu HY, Stern A and Chiu DT: Glucose-6-phosphate dehydrogenase, redox homeostasis and embryogenesis. Int J Mol Sci 23: 2017, 2022.
38. He F, Ru X and Wen T: NRF2, a transcription factor for stress response and beyond. Int J Mol Sci 21: 4777, 2020.
39. Sun YY, Zhu HJ, Zhao RY, Zhou SY, Wang MQ, Yang Y and Guo ZN: Remote ischemic conditioning attenuates oxidative stress and inflammation via the Nrf2/HO-1 pathway in MCAO mice. Redox Biol 66: 102852, 2023.
40. Liu J, Huang C, Liu J, Meng C, Gu Q, Du X, Yan M, Yu Y, Liu F and Xia C: Nrf2 and its dependent autophagy activation cooperatively counteract ferroptosis to alleviate acute liver injury. Pharmacol Res 187: 106563, 2023.
41. Wang YY, Chen J, Liu XM, Zhao R and Zhe H: Nrf2-mediated metabolic reprogramming in cancer. Oxid Med Cell Longev 2018: 9304091, 2018.
42. Alonso-Piñeiro JA, Gonzalez-Rovira A, Sánchez-Gomar I, Moreno JA and Durán-Ruiz MC: Nrf2 and heme oxygenase-1 involvement in atherosclerosis related oxidative stress. Antioxidants (Basel) 10: 1463, 2021.
43. Fiorelli S, Porro B, Cosentino N, Di Minno A, Manega CM, Fabbiocchi F, Niccoli G, Fracassi F, Barbieri MS, Marenzi G, *et al*: Activation of Nrf2/HO-1 pathway and human atherosclerotic plaque vulnerability:An in vitro and in vivo study. Cells 8: 356, 2019.